Microbiome

RESEARCH

Open Access

Microbial mechanisms for higher hydrogen production in anaerobic digestion at constant temperature versus gradient heating

Heng Wu[1], Anjie Li[2], Huaiwen Zhang[1], Suqi Li[3], Caiyun Yang[3], Hongyi Lv[1] and Yiqing Yao[1*]

Abstract

Background Clean energy hydrogen (H_2) produced from abundant lignocellulose is an alternative to fossil energy. As an essential influencing factor, there is a lack of comparison between constant temperatures (35, 55 and 65 °C) and gradient heating temperature (35 to 65 °C) on the H_2 production regulation potential from lignocellulose-rich straw via high-solid anaerobic digestion (HS-AD). More importantly, the microbial mechanism of temperature regulating H_2 accumulation needs to be investigated.

Results Constant 65 °C led to the lowest lignin residue (1.93%) and the maximum release of cellulose and hemicellulose, and the highest H_2 production (26.01 mL/g VS). H_2 production at 35 and 55 °C was only 14.56 and 24.13 mL/g VS, respectively. In order to further explore the potential of ultra-high temperature (65 °C), HS-AD was performed by gradient heating conditions (35 to 65 °C). However, compared to constant 65 °C, gradient heating conditions led to higher lignin residue (2.49%) and lower H_2 production (13.53 mL/g VS) than gradient heating conditions (47.98%). In addition, metagenomic analysis showed the cellulose/hemicellulose hydrolyzing bacteria and genes (mainly *Thermoclostridium*, and *xynA, xynB, abfA, bglB* and *xynD*), H_2-producing bacteria and related genes (mainly *Thermoclostridium*, and *nifD*, *nifH* and *nifK*), and microbial movement and metabolic functions were enriched at 65 °C. However, the enrichment of two-component systems under gradient heating conditions resulted in a lack of highly-enriched ultra-high-temperature cellulose/hemicellulose hydrolyzing genera and related genes but rather enriched H_2 consumption genera and genes (mainly *Acetivibrio,* and *hyaB* and *hyaA*) resulting in a weaker H_2 production.

Conclusions The lignin degradation process does not directly determine H_2 accumulation, which was actually regulated by bacteria/genes contributing to H_2 production/consumption. In addition, it is temperature that enhances the hydrolysis process of lignin rather than lignin-degrading enzymes, bacteria and genes by promoting microbial material transfer and metabolism. In terms of temperature, one of the key parameters of HS-AD for H_2 production, we developed an important regulatory strategy, enriched the theoretical basis of temperature regulation for H_2 production to further expanded the research horizon in this field.

Keywords High-solid anaerobic digestion, Hydrogen, Metagenomics, Temperature

*Correspondence:
Yiqing Yao
dzhtyao@nwafu.edu.cn; dzhtyao@126.com
Full list of author information is available at the end of the article

Background

With the increasing use of fossil fuels, the world is facing increasingly severe energy depletion and environmental pollution, so the use and promotion of renewable energy are particularly important [1]. In recent years, biomass resources rich in lignocellulose have attracted wide attention due to their abundant reserves, wide application scope and renewable characteristics [2]. Global lignocellulose biomass production is about 200 Gt annually, mainly from the agricultural field, including wheat straw, rice straw, rice husk, wheat straw (WS), cotton seeds, maize straw, maize leaves, garden waste, pine and maple [3]. In 2015, China's crop straw accounted for more than 3‰ of the global total, and this proportion has been increasing annually, is one of the most abundant biomass resources in the world [4]. Biomass can be converted into clean energy with high heat energy by anaerobic digestion (AD), such as for hydrogen (H_2) production. H_2 has clean combustion products and a high calorific value (142 kJ/g), which not only avoids the pollution of the environment but also does not emit greenhouse gases [5]. Therefore, H_2 production from WS via AD is a clean energy production approach with broad prospects.

According to the total solid (TS) concentration, AD can be divided into liquid-state anaerobic digestion (LS-AD) and high-solid anaerobic digestion (HS-AD) [6]. Compared to LS-AD, the higher heat produced in HS-AD can promote the biological reaction process, and higher TS concentration leads to higher gas production [7]. More importantly, HS-AD cannot only save water resources, but also avoid high costs caused by postprocessing the large discharge of biogas slurry, which is more suitable for application in water shortage areas [8]. Therefore, HS-AD is a potential and important resource utilization way in arid and semiarid areas. However, the lignocellulose composed of cellulose, hemicellulose and lignin can significantly affect the hydrolysis process, which is the rate-limiting factor of AD [9]. In order to promote the degradation of agricultural straws, some physical, chemical and biological methods have been taken by researchers, such as adding activated carbon [10], formic acid dehydrogenation treatment [11], adding hydrolysis enzymes [12] and construction of synthetic microbial consortia [13]. Temperature is a key factor affecting microbial activity and biological reaction processes. Previous studies have shown that temperature affects the microbial community composition and the conversion efficiency of the substrate to H_2, and temperature regulation is more economical than other methods [14]. High temperature (55 °C) can reduce the viscosity of the HS-AD system and improve the mass transfer efficiency than medium temperature (35 °C), resulting in a faster hydrolysis rate and higher H_2 production [15]. Some studies even confirmed that ultra-high temperature (65 °C) can promote the hydrolysis and acidogenic process better than 55 °C [16]. In addition, the inability of methanogenic archaea to survive under ultra-high-temperature conditions leads to lower H_2 consumption, which makes more H_2 production [17]. However, there are few comprehensive studies on the effects of various constant temperatures (35, 55 and 65 °C) on H_2 production from lignocellulosic materials, not to mention in the HS-AD system. More importantly, the effect of gradient heating conditions on H_2 production from lignocellulosic materials is still unknown. Theoretically, gradient heating from 35 to 65 °C can promote the activity of cellulase and hemicellulase and inhibit the process of methanogenic process, which has more potential for H_2 production than under constant temperature. In addition, the domestication of microbial communities by gradient heating conditions might also lead to more hydrolyzing bacteria being completely retained and highly enriched with the increase in temperature, which will promote the hydrolysis process. However, this speculation remains to be verified.

Based on the above, this study used WS as a representative of lignocellulosic substrate for H_2 production by HS-AD. The H_2 production performance under different constant temperatures (35, 55 and 65 °C) was evaluated. The H_2 production potential under an optimal condition obtained from the three constant temperature condition was further compared to that under gradient heating conditions. Also, the lignocellulose degradation characteristics under different temperatures were studied by crystallinity calculation, functional group analysis and enzyme activity determination, and the key factor for strongly promoting H_2 production was identified. In addition, metagenomic analysis was used to reveal the mechanism of the key factors regulating the metabolism of the functional microorganisms involved in H_2 production. This study has potential to provide new insights for efficient H_2 production from lignocellulosic materials via HS-AD by regulating temperature.

Materials and methods

Waste activated sludge and straw

The waste activated sludge (WAS) was obtained from a wastewater treatment plant in Yangling District, Shaanxi Province. Tap water was added to adjust the TS and volatile solid (VS) to 4.30% and 2.30%, respectively. The total carbon (TC) and total nitrogen (TN) of the dried WAS were determined to be 23.13% and 3.11%, respectively. The TS and VS of WS were 89.36% and 77.05%, respectively. The TC and TN of dried WS were determined to be 37.20% and 0.72%, respectively. The pH of WAS was 8.80.

Experimental procedure

The 500-mL fermenter was used for HS-AD. The TS of AD system used for WS and WAS was about 11%, with an initial operating volume of 350 mL. WAS was used as an inoculum because its rich microorganisms that can adapt to different temperatures (including 35 and 65 °C) [18, 19]. Fermenters were placed in four temperatures (constant 35, 55 and 65 °C, and a gradient from 35 to 65 °C), and each temperature condition was applied to three parallel groups. The constant 35 °C medium-temperature, 55 °C high-temperature, and 65 °C ultra-high-temperature groups are designated as MG, HG and UG for the purpose of this report. The 35 to 65 °C gradient groups (designated GG) were heated from 35 to 65 °C increasing by 5 °C increments every 12 h, before being maintained at a constant 65 °C. Samples were taken from all fermenters every 2 days to measure NH_4^+-N, chemical oxygen demand (COD), methane (CH_4), electric conductivity (EC) and volatile fatty acid (VFA) with pH adjusted to about 10 by addition of 6 mol/L NaOH.

Enzyme activity assessment in AD systems

The activity of lignin degradation process was evaluated by measuring lignin esterase (LE) activity [20], respectively. Given that protease is the key enzyme in protein hydrolysis, and acetate kinase (AK) [21] and [FeFe] hydrogenase (Hase) [22] in acetogenic and H_2 production, respectively, their activity was also assayed. For all groups, enzyme activities were determined before and after HS-AD.

DNA extraction, metagenome sequencing and annotations

The biofilms collected in MG, HG, UG, GG are named as MG, HG, UG, and GG, respectively. The unfermented initial sample is named the original sample (OS). Total DNA was extracted and metagenomic analyses were performed by Majorbio Bio-Pharm Technology Co., Ltd. (Shanghai, China). All the measurements were performed in triplicate. Total genomic DNA was extracted from these samples using the Mag-Bind® Soil DNA Kit (Omega Bio-tek, Norcross, GA, USA). Concentration and purity of extracted DNA was determined using TBS-380 and NanoDrop2000, respectively. To construct paired-end libraries, the DNA extract was fragmented to an average size of approximately 400 bp using the Covaris M220. The NEXTFLEX Rapid DNA-Seq kit (Bioo Scientific, Austin, TX, USA) was used for the library construction. Adapters containing the necessary sequencing primer hybridization sites were ligated to the blunt ends of the DNA fragments. Paired-end sequencing was performed on Illumina NovaSeq (Illumina Inc., San Diego, CA, USA) at Majorbio Bio-Pharm Technology Co., Ltd. using NovaSeq 6000 S4 Reagent Kit v1.5 (300 cycles). Representative sequences of non-redundant gene catalog were aligned to NR database with an e-value cutoff of 1e-5 using Diamond (http://www.diamondsearch.org, version 0.8.35) for taxonomic annotations. Functional annotation of metagenomes was performed using a BLASTP search against the KEGG database (http://www.genome.jp/kegg) with an E-value cutoff of ≤ 10 to 5.

Analytical methods

The COD and NH_4^+-N were determined by the standard method [23]. TC and TN were measured by the elemental analyzer (Elementar vario MACRO cube, Germany). The TS and VS were measured by the weight loss method [24]. pH is measured with a pH meter (PHS-3C, China). Determination of VFA and CH_4 was as previously described, and total VFA was calculated as the values for acetic, propionic, n-butyric, isobutyric, n-valeric and isovaleric acids [25]. The concentration of LE, protease, AK, and Hase were analyzed with a kit from Shanghai Enzyme-linked Biotechnology Co., Ltd (Shanghai, China) according to the manufacture's instructions. Lignin, cellulose and hemicellulose were measured according to published methods [26]. EC was measured by a conductivity meter (Youke conductivity DDS-11A, China). Crystallinity, expressed as crystallinity index (*CrI*), was determined using a powder X-ray diffractometer (XRD) (Bruker D8 Advance A25, Germany) with Cu radiation at 40 kV and 40 mA. Samples were scanned in the 2θ range of 5° to 50°. The *CrI* was calculated as:

$$CrI = [(I_{002} - I_{am})/I_{002}]/100, \quad (1)$$

where I_{002} is the maximum crystalline diffraction intensity of cellulose I at 22° to 23° (for cellulose II, 2θ is 18° to 22°) and I_{am} is the crystalline diffraction intensity of cellulose I at 2θ of 18° to 19° (for cellulose II, 2θ is 13° to 15°). Fourier transform infrared spectroscopy (FT-IR) (Vertex70, Germany) was used to investigate organic functional groups and structural changes in fermenters. Spectra were recorded between 4000 and 500 cm^{-1}.

Results and discussion

HS-AD performance

In order to compare the effects of HS-AD temperatures on H_2 production performance, the performance of each stage involved in the process was evaluated. COD is an important indicator representing hydrolytic performance. As shown in Fig. 1a, the initial COD was about 14,707.69 mg/L, and the COD in MG, HG, UG and GG increased gradually from the first to sixth day, reaching the highest values of 31,443.59, 31,705.13, 29,141.03 and 27,666.67 mg/L on the sixth day, respectively. However, the subsequent COD did not continue to increase,

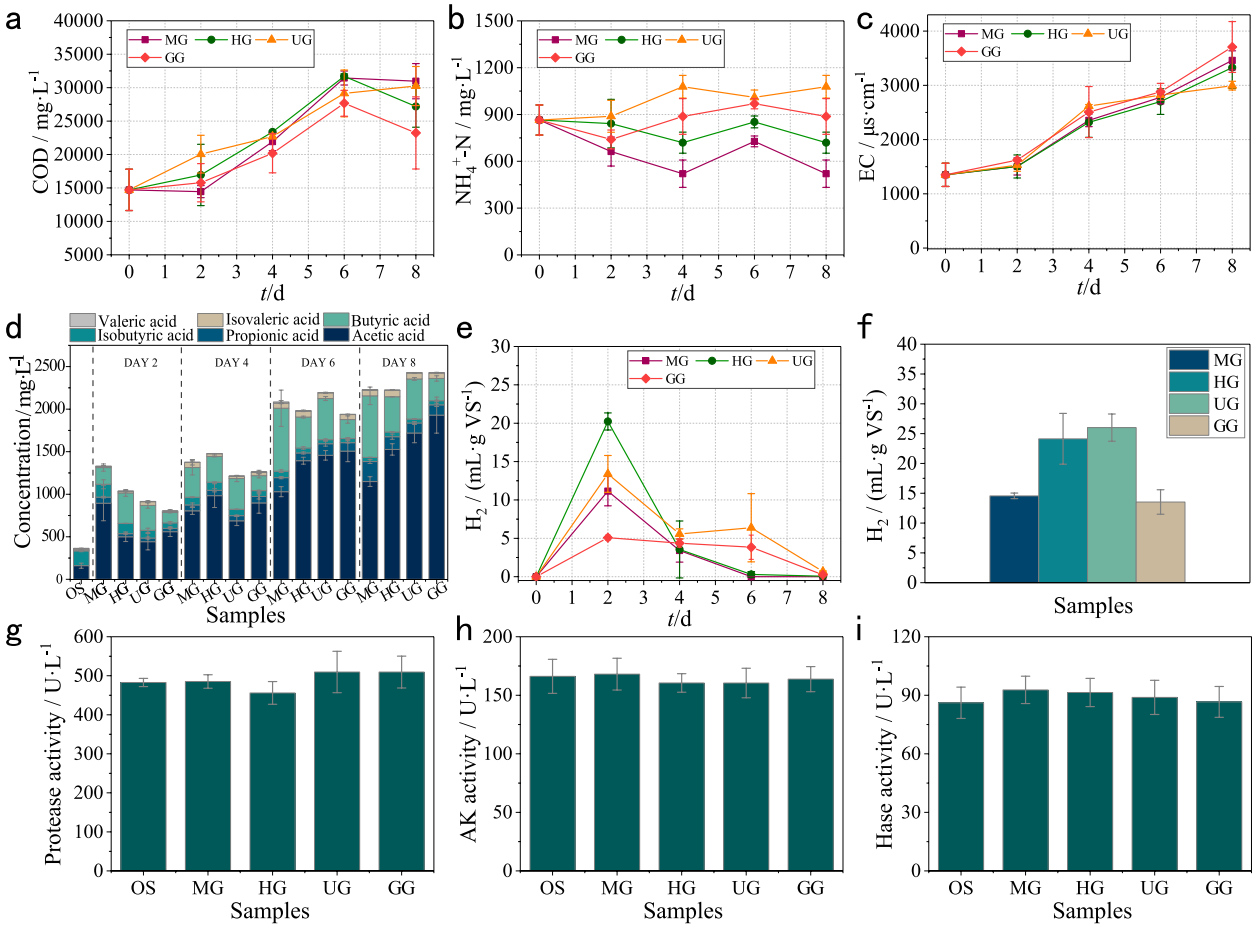

Fig. 1 AD performance under different temperature conditions during HS-AD. **a** COD concentration, **b** NH_4^+-N concentration, **c** Electrical conductivity, **d** VFAs concentration, **e** Daily H_2 production, **f** Cumulative H_2 production, **g** Protease activity, **h** AK activity, and **i** Hase activity

and they were only 30,969.23, 27,180.77, 30,246.15 and 23,230.77 mg/L on eighth day, respectively. This could be due to the large of COD during the peak period of hydrolysis, while the continuous consumption of organic matter leads to a decrease in COD when the hydrolysis slows down or almost ends. The hydrolytic performance of HG was similar to MG, but HG consumes more organic matter. Compared to MG, and HG, the COD of UG kept increasing, indicating that the hydrolytic performance at 65 °C was superior and more stable. Compared to UG, the COD of GG was consistently lower, indicating that GG conditions resulted in a lower hydrolytic performance. Therefore, the HS-AD hydrolytic performance of UG was better than that of GG.

Some soluble salts were gradually released as the hydrolysis proceeded. The measured EC indicates the soluble salt concentration released during the hydrolysis process, and an appropriate concentration can maintain stable osmotic pressure and assist the metabolic process of microorganisms [27]. As shown in Fig. 1c, the EC of the OS was 1349.75 μS/cm, and on the eighth day of HS-AD, the EC in MG, HG, UG and GG increased to 3460.00, 3326.67, 2993.33, and 3706.67 μS/cm on the eighth day, respectively. Of the constant temperature conditions, UG was lower than MG and HG on the eighth day, indicating that microorganisms in UG had more stable osmotic pressure. A higher EC in GG was also detected than in UG, indicating that microbial stability in GG was inferior. Also, the NH_4^+-N concentration mostly fluctuates due to the decomposition of protein and other organic matter. As shown in Fig. 1b, the initial NH_4^+-N concentration was 864.64 mg/L, then the NH_4^+-N concentration in MG and HG gradually decreased to 520.54 and 719.40 mg/L, respectively, while in UG it rose to 1077.99 mg/L. Similar to the trend of UG, the NH_4^+-N concentration in GG rose to 887.33 mg/L. Although GG also detected a continuous increase in NH_4^+-N concentration, it was lower than that of UG, indicating that UG had superior hydrolytic performance. This confirms the conclusion evident in Fig. 1a.

Subsequently, the acidogenic performance was analyzed in Fig. 1d. The VFA of OS was 364.63 mg/L. As the AD progressed, the VFA concentrations in MG, HG, UG, and GG gradually increased to 2228.47, 2224.16, 2429.03, and 2427.81 mg/L on the eighth day, respectively. The continued increase in VFA concentration indicated that the acidogenic process was proceeding smoothly. In addition, the composition of VFA showed that the proportion of acetic acid produced by MG decreased from 67.21% on the second day to 51.55% on the eighth day, while the proportion of acetic acid under the conditions of HG, UG and GG increased from 48.23%, 48.33% and 69.72% on the second day to 68.63%, 70.79%, and 79.48% on the eighth day, respectively. Although the VFA concentrations of MG and HG were higher in the first 4 days, UG gave superior acidogenic performance in the next four days, and a higher acetic acid production ratio also indicated that UG had superior acetogenic performance. Among the constant temperature conditions, the acidogenic performance was in the order, UG > HG > MG. Compared to UG, GG had similarly high acidogenic and acetogenic performance. During HS-AD, superior acidogenic and acetogenic performance was achieved with both UG and GG.

Further, the H_2 production performance was analyzed (Fig. 1e). On the second day of AD, H_2 production peaked in MG, HG, UG, and GG at 11.215, 20.23, 13.439, and 5.08 mL/g VS, respectively. As shown in Fig. 1f, after 8 days, the cumulative H_2 production were 14.56, 24.13, 26.01, and 13.53 mL/g VS, respectively. The order of cumulative H_2 production was consistent with the trend in acidogenic performance, that is, UG > HG > MG. Compared to UG, the daily H_2 production and cumulative H_2 production of GG were lower. Therefore, the hydrolysis, acidogenic and H_2 production of HS-AD under constant temperature increase with temperature. However, it is surprising that although Fig. 1d shows that the acidogenic process under GG has advantages, Fig. 1a and e show that its hydrolysis and H_2 production performance were inferior to UG. Thus, hydrolysis must have a decisive role in the processes leading to H_2 production.

What are the reasons for the phenomenon? The hydrolysis, acidogenic and H_2 production processes were directly regulated by functional enzymes, so the activities of protease, AK and Hase were evaluated. The sludge as an inoculum contains proteins, and the activity of the sludge hydrolysis process could be evaluated by measuring protease activities. As shown in Fig. 1g, the protease activity in OS was 482.74 U/L, and it changed to 485.30, 456.00, 509.62 and 509.48 U/L after HS-AD, respectively. UG had higher protease activity than MG and HG, indicating that 65 °C was more conducive to protein hydrolysis. Although GG had similarly high protease activity, the low hydrolytic performance indicated that protein hydrolysis might not be the main factor determining the hydrolytic performance instead of lignocellulose degradation. The hydrolysis is followed by an acidogenic process. As shown in Fig. 1h, the AK activity in OS was 166.18 U/L, and the AK in MG, HG, UG and GG reached 168.30, 160.51, 160.47 and 163.78 U/L after HS-AD, respectively. Notably, the trends for AK activity and acetogenic performance are opposite. The AK activity in UG was lower than in HG and MG, indicating that its high yield of acetic acid could be attributed to high hydrolytic performance and the efficient biochemical reaction process caused by ultra-high temperature. The AK activity in GG was similar to that in UG, but high acetic acid was obtained with low hydrolytic performance. The reason could be that to the acidogenic pathway is enriched under gradient heating conditions. Hase is the key enzyme producing H_2, as shown in Fig. 1i, Hase activity in OS was 86.15 U/L, and Hase activity in MG, HG, UG and GG reached 92.76, 91.43, 88.92 and 86.61 U/L during HS-AD, respectively. Among constant temperature conditions, Hase activity was opposite to H_2 production, which indicates that H_2 production might be determined by hydrolytic performance. The low hydrolytic performance of GG confirmed this conclusion. Although the acidogenic performance was superior, limited organic matter was hydrolyzed to produce less H_2.

Therefore, under constant temperature, the hydrolysis, acidogenic and H_2 production performance of UG was better than for MG and HG. Due to the higher hydrolytic performance, UG also had higher H_2 production than GG. The restrictive factor of the hydrolysis stage was lignocellulose degradation.

Lignocellulose degradation

In order to further analyze constraints to the hydrolysis process under constant temperature and gradient heating conditions, the main components (cellulose, hemicellulose and lignin) of WS after AD were analyzed. Lignin is the key component to limiting WS degradation [28]. As shown in Fig. 2a, the proportion of lignin, hemicellulose and cellulose in the OS samples were 5.16%, 17.99%, and 27.17%, respectively. After HS-AD, the lignin contents of MG, HG, UG, and GG were 2.31%, 2.14%, 1.93% and 2.49%, respectively. It was worth noting that the degradation efficiency of lignin was consistent with the trend in hydrolytic performance, namely, UG > HG > MG. Also, the lignin degradation efficiency of GG was also lower than that of UG. Hemicellulose is an amorphous component that is easily hydrolyzed subsequently. Hemicellulose is closely bound to lignin by hydrogen bond and van der Waals forces, and is resistant to degradation. As lignin

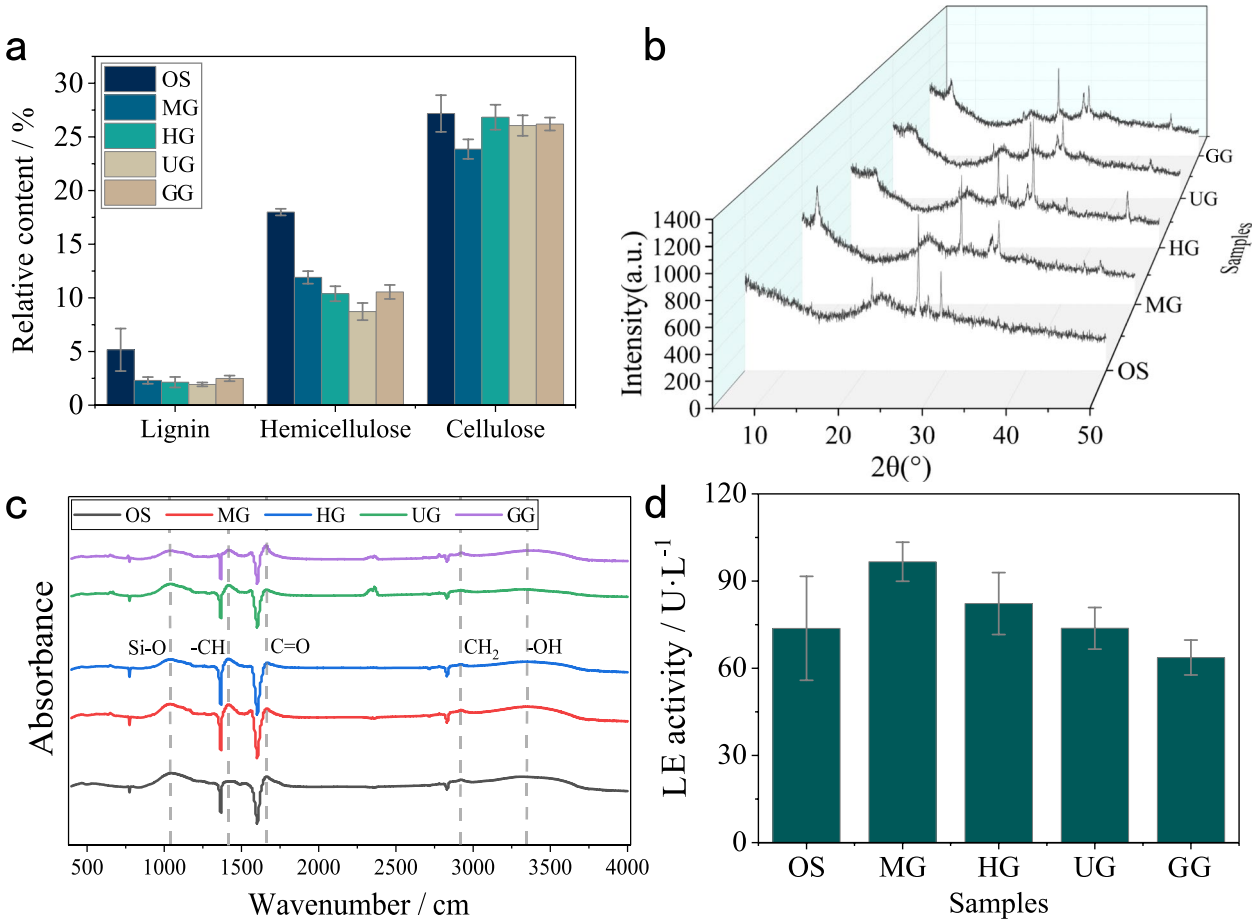

Fig. 2 Degradation characteristics of lignocellulose under different temperature conditions. **a** Lignocellulose degradation efficiency, **b** XRD of WS, **c** FT-IR of WS, and **d** LE activity

degradation, hemicellulose is degraded. The proportion of hemicellulose in MG, HG, UG and GG were 11.91%, 10.39%, 8.72% and 10.55%, respectively. Under constant temperature, the degradation rate of hemicellulose was consistent with that of lignin, and UG had the highest degradation performance. Compared to UG, the lignin degradation in GG was less, which indicates that the lignin degradation was positively correlated to subsequent hemicellulose degradation. The crystalline cellulose and hemicellulose are intertwined and degrade together. The cellulose contents of MG, HG, UG and GG were 23.86%, 26.83%, 26.05%, and 26.20%, respectively. The cellulose degradation performance of UG was better than that of HG, but not MG. In addition, compared to UG, GG has lower performance. This indicated that cellulose degradation might not be the main process determining hydrolytic performance, but rather it would be lignin degradation. The low cellulose degradation rate in all samples could be seen as consistent with this conclusion.

In order to analyze the limiting components of degradation process of cellulose, the crystallinity of cellulose was analyzed to evaluate the degradation characteristics of crystalline and the non-crystalline cellulose regions. As shown in Fig. 2b, the XRD patterns of OS, MG, HG, UG and GG were analyzed, and the crystallinity of cellulose I of each sample was calculated using Eq. 1 as 34.58%, 39.50%, 43.95%, 44.07% and 37.42%, respectively. The crystallinity of all samples increased during HS-AD, which was due to the high degradation effect of the non-crystalline region and the relatively lower degradation effect of crystallinity. The crystallinity of UG was higher than that of MG and HG, indicating that 65 °C was more conducive to the degradation of the non-crystalline region. The crystallinity of GG was lower than that of UG, indicating that not only lignin and hemicellulose but also the degradation performance of both non-crystalline region and crystalline region were lower under gradient heating conditions. Conversion of cellulose I to II could also lead to changes in crystallinity. In order to verify the

conclusions, the crystallinity of cellulose II was calculated using Eq. 1. The crystallinity of cellulose II of OS, MG, HG, UG and GG were 50.48%, 44.43%, 41.58%, 40.37%, and 37.42%, respectively, indicating that cellulose II was also degraded during AD, and there was no new cellulose II being converted from cellulose I. During AD, the non-crystalline region of cellulose was mainly degraded. Therefore, the lignin degradation process is the main factor leading to the hydrolytic performance differences between UG and GG, followed by cellulose and hemicellulose. The H_2 production performance of UG was better than that of MG and HG, which was also due to the high lignin degradation performance.

How is lignocellulose efficiently degraded at 65 °C? The degradation metabolite characteristic of lignin at different temperatures was revealed. The functional groups of the products in HS-AD were analyzed by FTIR spectroscopy in Fig. 2c. The presence of a broad peak near 3328 cm^{-1} due to the stretching vibration of -OH, and the absorption intensity in MG, HG, UG and GG was lower than in OS, indicating that the hydrogen bonds of lignin had been destroyed. Among the constant temperature conditions, the peaks of HG and MG were larger than those of UG, which confirmed that UG had superior degradation performance. Compared to UG, the peak of GG is more obvious, indicating that the degradation performance of GG was weaker than UG. The ultra-high temperature of UG was more conducive to splitting lignin and hemicellulose linked by hydrogen bonds, thereby releasing hemicellulose. The peak at 1666 cm^{-1} represents the carbonyl C=O stretching vibration between hemicellulose and lignin, and exists in carboxyl, aldehyde, ketone and ester groups. The peak at 1666 cm^{-1} after HS-AD was smaller than in OS, indicating that the lignin side chain had been broken. Compared to HG and MG, the change in the UG peak was the most obvious, indicating that the degradation performance of carboxyl, aldehyde, ketone and ester groups was the best at 65 °C. The peak of GG was also higher than that of UG, indicating that the degradation performance of these functional groups was poor under gradient heating conditions. In addition, the peak near 2919 cm^{-1} was attributed to CH_2 stretching vibration, and the low peak after HS-AD indicated that the methyl and methylene groups of cellulose were released and degraded. However, there was no substantive difference in the peaks of each sample, which confirmed the low cellulose degradation performance of HS-AD. The peak at 1384 cm^{-1} was contributed to -CH stretching vibration in cellulose and hemicellulose. The peak became larger after HS-AD, which could be due to the higher proportion of residual cellulose in these samples.

Why the best lignin degradation performance was obtained at 65 °C? The degradation of lignocellulose is directly regulated by functional enzymes. Therefore, the activity of functional enzymes under different temperature conditions was evaluated. As shown in Fig. 2d, LE is the key functional enzyme for lignin degradation. LE activity in OS was 73.73 U/L. After HS-AD, the LE activities in OS, MG, HG, UG and GG were 96.64, 82.27, 73.75 and 63.69 U/L, respectively. The higher the temperature, the lower the LE activity under constant temperature, with UG having the lowest LE activity. LE activity was not consistent with hydrolytic performance, which indicated that LE activity was not the main determinant of hydrolytic performance. Compared to UG, the lower LE activity of GG confirmed that gradient heating conditions were not conducive to lignin hydrolysis. Therefore, the low LE activity at 65 °C was also not the main reason for the high lignin degradation efficiency.

Therefore, the constant 65 °C promoted the deconstruction of the hydrogen bond, carboxyl, aldehyde, ketone and ester groups of lignin, so that hemicellulose and cellulose wrapped by lignin could be released, and then efficient utilized. However, the LE activity was not the key factor limiting lignin hydrolysis, which needed to be further explained by functional bacteria.

Microbial community structure

Temperature variations will affect the microbial community structure, and continuous heating even can directly drive the reconstruction of microbial community structure. The change of microbial community structure is closely related to the degradation rate of lignocellulose. In order to reveal the key mechanisms determining lignocellulose hydrolysis, we focused on the dynamic changes of the hydrolytic microbial communities, and undertook detailed identification of hydrolytic bacteria based on metagenomic sequencing to genus level where possible. Also, in order to fully reveal the limiting factors of H_2 production, H_2-producing/consuming bacteria were also identified. As shown in Fig. 3, the bacteria with lignin, cellulose and hemicellulose degradation genes were identified. The dominant microbial genus in OS was denitrifying bacteria. For example, the abundance of *Rhodococcus* [29] was as high as 11.60%. In addition, subdominant bacteria were identified as cellulose degrading taxa [*Mycolicibacterium* (4.46%), *Mycobacterium* (4.20%), *Bradyrhizobium* (2.45%), *unclassified_Acidobacteria* (1.04%) and *Pseudoxanthomonas* (1.26%)], and a hemicellulose degrading genus *Amaricoccus* (1.70%). There were also a lignin/cellulose-degrading taxon identified as *unclassified_Candidatus Hydrogenedentes* (2.14%) and cellulose/hemicellulose-degrading taxa [*Hyphomicrobium* (1.65%), *Mesorhizobium* (1.51%), *Thiobacillus* (1.02%), *Rhodovulum* (0.96%) and *unclassified_Proteobacteria* (0.94%)],

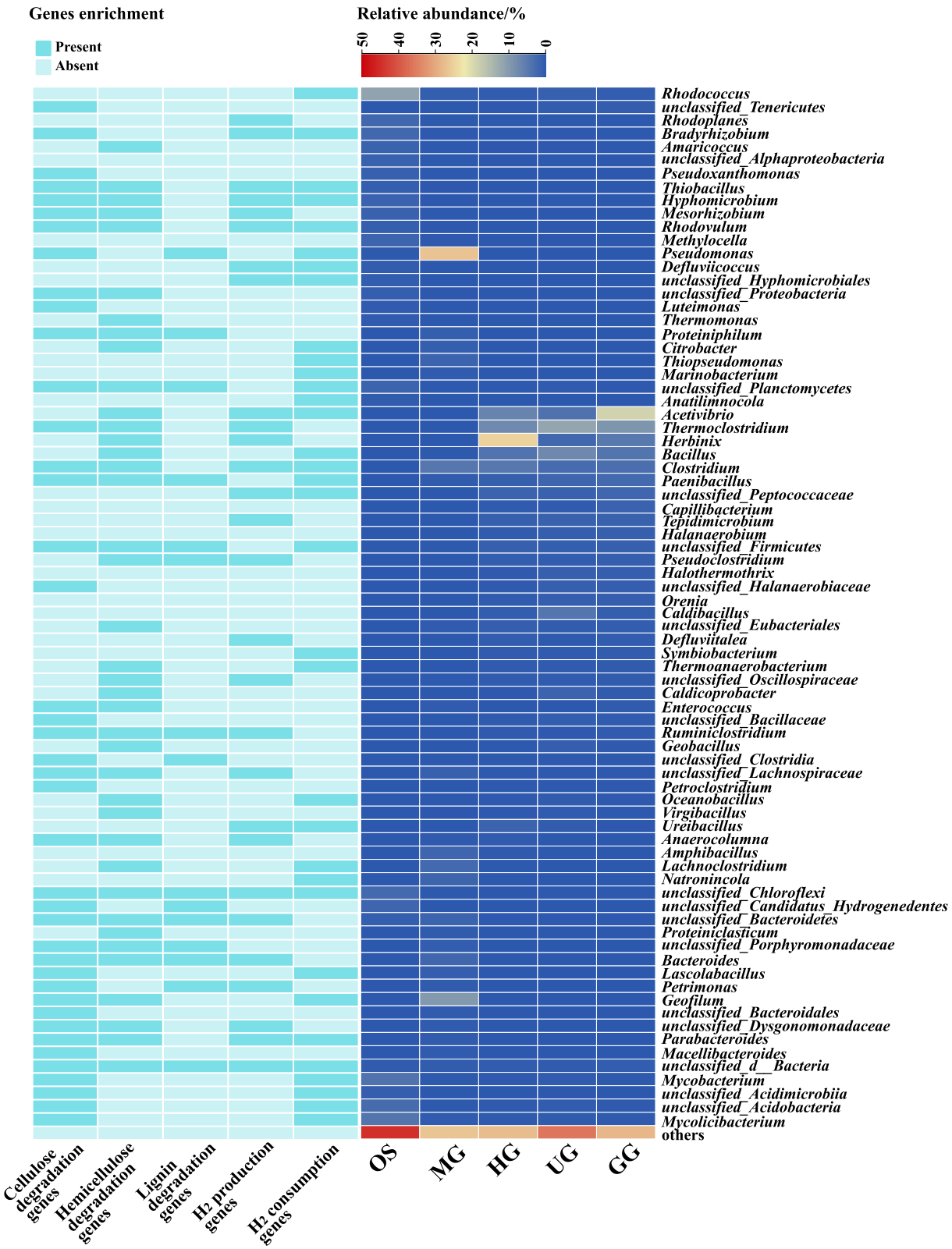

Fig. 3 The abundance of bacteria with lignocellulose degradation genes and genes involved in H_2 production and consumption processes at different temperatures

and lignocellulose-degrading taxa [*unclassified_Chloroflexi* (2.66%), *unclassified_Planctomycetes* (1.81%) and *unclassified_Bacteroidetes* (0.98%)]. Although these taxa carry hydrolysis genes, they have also been reported as acidogenic, such as *unclassified_Acidimicrobiia* [30], *unclassified_Candidatus_Hydrogenedentes* [31] and *unclassified_Bacteroidetes* [32]. However, almost all the dominant genera in OS had H_2 consumption-related genes, including *Rhodococcus*, *Mycolicibacterium*, *Mycobacterium* and *unclassified_Acidobacteria*. Therefore, the main function of the microbial communities was denitrification and H_2 consumption, followed by hydrolysis and acid production.

The microbial community structure in MG changed significantly. The key dominant genus *Rhodococcus* was replaced by the lignin/cellulose-degrading genus *Pseudomonas* (27.00%). The subdominant bacteria were cellulose/hemicellulose-degrading taxa [*Geofilum* (10.106%), *Clostridium* (4.78%), *unclassified_Lachnospiraceae* (1.26%) and *Parabacteroides* (0.66%)], hemicellulose-degrading genera [*Lachnoclostridium* (2.70%) and *Citrobacter* (0.94%)] and lignocellulose-degrading taxa [*Bacteroides* (2.37%), *unclassified_Bacteroidetes* (1.76%), *Proteiniphilum* (0.96%), *unclassified_Porphyromonadaceae* (0.89%) and *Paenibacillus* (0.67%)]. *Lachnoclostridium* [33], *Bacteroides* [34], *Proteiniphilum* [35] and *Natroniincola* (2.05%) [36] have been reported as acid-producing genera. However, only *Thiopseudomonas* (1.82%), that does not carry hydrolysis genes, has been detected as high abundance genus involved in denitrification [37]. This indicated that the enrichment of hydrolytic and acidogenic genera in MG had occurred, and the genera involved in denitrification were secondary. Also, the taxa with H_2 production-related genes in MG were detected, including *Clostridium*, *Bacteroides* and *unclassified_Bacteroidetes*. However, the key dominant genera almost all had H_2 consumption-related genes, including *Pseudomonas*, *Geofilum* and *Lachnoclostridium*. This explains why the high abundance of *Pseudomonas* in MG resulted in low H_2 production.

The microbial community in HG was dominated by hydrolytic and H_2-producing bacteria. The main dominant bacteria were in the hemicellulose-degrading genus *Herbinix* (25.10%). The subdominant bacteria were in hemicellulose-degrading taxa [*Acetivibrio* (6.78%), *Bacillus* (4.24%), *unclassified_Eubacteriales* (1.07%), *Thermoanaerobacterium* (0.50%) and *unclassified_Oscillospiraceae* (0.50%)], cellulose/hemicellulose-degrading genera [*Thermoclostridium* (7.70%) and *Clostridium* (5.50%)], a lignin/hemicellulose-degrading genus *Pseudoclostridium* (0.91%) and lignocellulose-degrading taxa [*Paenibacillus* (1.24%) and *unclassified_Firmicutes* (1.22%)]. Among these, *Paenibacillus* [38], *Pseudoclostridium* [39] and *unclassified_Peptococcaceae* (1.77%), [40] and *Tepidimicrobium* (1.24%) [41] without hydrolysis genes, have been reported as acidogenic taxa. Although the function of the microbial community is mainly hydrolysis, acid production and H_2 production, the structure changed significantly. All the hydrolytic bacteria given above were considered to be the dominant genera, which belonging to the phylum Firmicutes with high or ultra-high-temperature resistance [42]. These genera were not highly enriched in OS and MG, but were in HG, indicating that the genera suitable to 35 °C were gradually replaced by genera with higher temperature resistance. In addition, it was worth noting that most of these dominant genera carried cellulose and hemicellulose degradation genes, rather than lignin degradation genes, indicating that the abundance of lignin-degrading bacteria, decreased during temperature-driven community reconstruction. The trend to enrichment of lignin-degrading bacteria was obviously not consistent with hydrolytic performance, which indicated that the hydrolytic performance might not be mainly determined by the lignin-degrading bacteria. In addition, the abundance of bacteria with H_2 production-related genes in HG was higher than that in MG, including *Herbinix* and *Thermoclostridium*. These were the key dominant genera occurring at high abundance. There were only subdominant bacteria that had H_2 consumption-related genes, including *Acetivibrio*, *Clostridium* and *Bacillus*. This explains why HG had higher H_2 production than MG. Compared with the low abundance of lignin-degrading bacteria, the enrichment of H_2-producing bacteria could be the main reason for H_2 accumulation.

The main dominant bacterial genera of UG were also in the Firmicutes. The microbial community was dominated by cellulose/hemicellulose degrading genus *Thermoclostridium* (11.89%). The genera with lignin degradation genes were also replaced by other genera. The subdominant bacteria were hemicellulose degrading genera [*Bacillus* (7.66%), *Acetivibrio* (4.09%), *Herbinix* (2.51%), *Caldicoprobacter* (1.88%) and *Geobacillus* (1.11%)], cellulose degrading taxa [*unclassified_Halanaerobiaceae* (1.24%), *unclassified_Bacillaceae* (0.82%) and *unclassified_Tenericutes* (0.79%)], the cellulose/hemicellulose degrading genus *Clostridium* (3.06%), the lignin/hemicellulose degrading genus *Pseudoclostridium* (0.76%), and cellulose degrading taxa [*Paenibacillus* (2.14%) and *unclassified_Firmicutes* (1.03%)]. Of these, *Thermoclostridium* [43], *Paenibacillus* [38] and *Caldicoprobacter* [39] have been reported as acidogenic genera. *Tepidimicrobium* (1.52%), *unclassified_Peptococcaceae* (1.14%), *Halothermothrix* (1.20%) and *Orenia* (1.10%) were also considered to be important in acidogenic process. The high abundance of acidogenic bacteria confirms the superior acid-producing performance evident in Fig. 1. With the increase of temperature, the characteristics of community composition driven by high temperature become

more obvious. *Thermoclostridium* further replaced *Herbinix*, and similarly *Bacillus* and *Paenibacillus* increased. Ultra-high-temperature as the selection pressure of the environment selected specific bacteria in the Firmicutes, indicating that *Thermoclostridium* was the main ultra-high-temperature resistant hydrolytic genus. The low abundance of lignin-degrading bacteria confirmed that the superior hydrolytic performance of UG might not be mainly regulated by bacterial abundance, but rather by the ultra-high-temperature. However, the decrease in the abundance of hydrolytic bacteria did not mean that the abundance of hydrolytic genes decreased, so this needs to be explained along with gene abundance. Also, H_2-producing bacteria were more enriched in UG. The key dominant genus *Thermoclostridium* was found to have H_2 production-related genes, along with *Clostridium* and *Herbinix*. Only low abundance of H_2 consumption genus (such as *Acetivibrio*) was detected. Therefore, high abundance of H_2-producing bacteria and low abundance of H_2-consuming bacteria could be the main cause of H_2 accumulation in UG.

The microbial community in GG was different from that in UG. The GG microbial community was dominated by hemicellulolytic genus *Acetivibrio* (18.91%) of the Firmicutes. The subdominant bacteria are cellulose/hemicellulose degrading genera [*Thermoclostridium* (9.45%) and *Clostridium* (3.65%)], hemicellulose degrading taxa [*Herbinix* (5.08%), *Bacillus* (4.48%) and unclassified Eubacteriales (0.85%)], cellulose-degrading taxa [*unclassified_Halanaerobiaceae* (1.07%) and *unclassified_Tenericutes* (0.92%)] and lignocellulose-degrading taxa [*Paenibacillus* (2.68%) and *unclassified_Firmicutes* (1.20%)]. *Thermoclostridium*, *Paenibacillus*, *Pseudoclostridium*, unclassified_*Peptococcaceae* (2.22%), *Tepidimicrobium* (1.44%), *Halothermothrix* (1.09%) [44] have been reported as acidogenic genera. The genera with lignin-degrading genes were still low in abundance. It was worth noting that, under gradient heating conditions, the abundance of the dominant genera *Thermoclostridium* and *Bacillus* found in UG decreased, while the abundance of *Acetivibrio* and *Herbinix* found in HG increased, indicating that the low environmental selection pressure in GG resulted in the enrichment of non-thermotolerant bacteria, which led to the reduction of the abundance of ultra-high-temperature tolerant hydrolytic bacteria. This was the main reason for the low hydrolytic performance of GG at 65 °C. Also, *Acetivibrio*, the key H_2-producing bacteria in GG, has also been confirmed to carry H_2 consumption-related genes, as well as *Bacillus*, *Paenibacillus* and *Clostridium*. In addition, only a low abundance of H_2-producing bacteria was detected, including *Thermoclostridium*, *Herbinix*, whose abundance was reduced. This indicates that the low accumulation of H_2 in GG could be caused by the enrichment of non-thermotolerant bacteria.

Therefore, under constant temperature, with the increase in temperature, H_2 production and ultra-high-temperature hydrolyzing bacteria were enriched, resulting in the highest hydrolytic performance and H_2 accumulation in UG. Compared to UG, gradient heating conditions of GG led to the enrichment of H_2-consuming bacteria and non-ultra-high-temperature hydrolyzing bacteria, resulting in a lower hydrolytic performance and decreased H_2 production. However, there are some questions that need to be explained and confirmed. 1) The enrichment of hydrolytic bacteria might not be the main factor determining the hydrolytic performance, with this conclusion needing to be confirmed through gene abundance. Also, it needs to be confirmed whether the temperature was the main factor affecting lignin hydrolysis. 2) Although it appeared that H_2-producing bacteria were the main factor affecting H_2 accumulation, it there is a need to further reveal gene abundance to confirm the effects of hydrolysis and H_2 production/consumption processes on H_2 accumulation. 3) In addition, what causes the low environmental selection pressure to functional bacteria in GG needs to be further understood.

Hydrolysis pathway and genes under different temperatures

Gene abundance is a key factor that directly affects microbial activity. To verify the effect of lignocellulose hydrolysis genes on hydrolytic performance and H_2 accumulation, we analyzed the lignin, cellulose, and hemicellulose degradation genes (Fig. 4). The gene *GE* encodes for lignin esterase and was enriched after HS-AD. The abundances of *GE* in OS, MG, HG, UG and GG were 0.20‰, 0.59‰, 0.05‰, 0.02‰ and 0.14‰, respectively. At constant temperature, with the increase in temperature, *GE* abundance decreased, which was consistent with the characteristics of its activity. Compared to GG, the *GE* abundance in UG was also lower. MG had the highest abundance of *GE* and the highest LE activity, which indicated that enzyme activity and gene abundance are not key limiting factors. Hemicellulose is also degraded with the deconstructed of lignin. Hydrolysis of the xylan backbone via the gene *xynA* encoding an endoxylanase produces short chains. The *xynA* abundances in OS, MG, HG, UG and GG were 0.141‰, 1.846‰, 2.207‰, 2.892‰ and 2.981‰, respectively. Further, *xynB* and *xylA*, encoding β-xylosidase that hydrolyzes short chains to produce xylose, reached the maximum abundance in UG at 1.234‰ and 0.002‰, respectively. The degradation of the xylan side chain also requires *abfA*, *xynD*, *abf1,* which encodes α-L-arabinofuranosidase that degrades the side chain through breaking the α-1,2, α-1,3

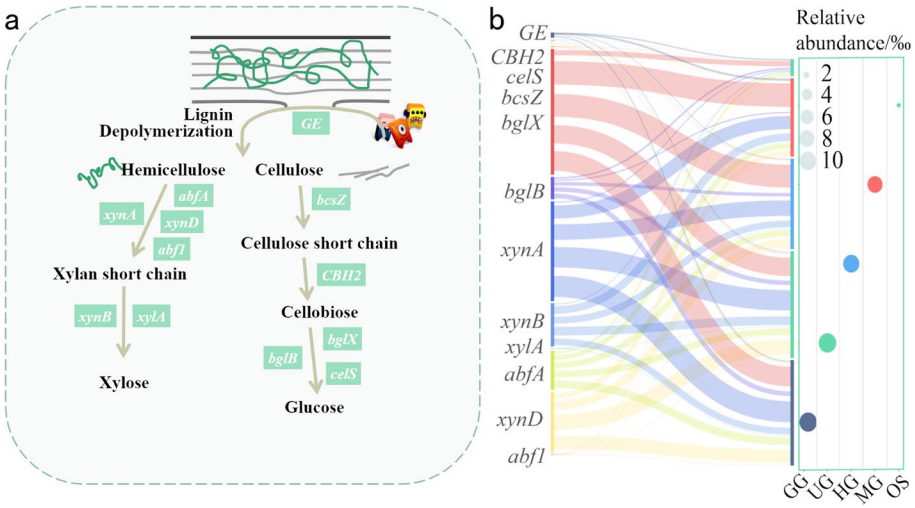

Fig. 4 The degradation mechanism diagram of lignocellulose. **a** Lignocellulose degradation steps and intermediate products, and **b** Abundance of genes involved in lignocellulose degradation

and α-1,5 bonds attached to the arabinose residue of the backbone. The abundance of *abf1* was lower after HS-AD than in OS, confirming that it was not a major functional gene. The abundances of *abfA* in GG and *xynD* in UG were the highest after HS-AD, at 1.111‰ and 2.192‰, respectively. These functional genes increased in abundance with increasing temperature, indicating that 65 °C was more likely to enrich functional genes involved in hemicellulose degradation, while the enrichment of these in GG was lower than that in UG. In general, cellulose is synergistically degraded with hemicellulose and lignin. The hydrolysis process first acts on the interior of cellulose through *bcsZ*, degrades long-chain cellulose into short chains and provides a reaction condition for cellobiohydrolase. The abundances of *bcsZ* in OS, MG, HG, UG and GG were 0.517‰, 1.996‰, 3.625‰, 3.040‰ and 3.838‰, respectively, indicating that it was enriched during AD, especially in GG. However, the activity of the encoded endoglucanase was low. Subsequently, cellobiose or cellotetraose was cleaved from the cellulose molecule to release cellodextrin and cellobiose. *CBH2* code for the enzyme responsible for the hydrolysis of (1- > 4)-β-D-glycosidic bonds in cellulose and cellotetraose, releasing cellobiose from the non-reducing end of the chain, and the abundance of *CBH2* in UG was the highest at 0.063‰. Finally, β-glucosidase further hydrolyzes cellobiose to produce glucose. The total abundance of *bglX* and *bglB*, which encode β-glucosidase, was the highest in MG and GG at 3.329‰ and 0.673‰, respectively. The highest abundance of *celS*, which coded for the enzyme responsible for the hydrolysis of cellulose 1,4-β-cellobiose, was 0.025‰ in HG. The genes involved in the initial cellulose cleavage were mainly enriched in UG and GG, while the genes involved in the subsequent degradation were enriched in MG and HG.

Therefore, the functional genes involved in cellulose/hemicellulose degradation were mainly enriched in UG and GG, followed by HG and MG, but the functional genes involved in lignin degradation were only enriched in MG. This conclusion addressed the questions 1) and 2) in Fig. 3, showing that the functional genus and genes involved in lignin degradation were not the main determinants of lignin hydrolysis and H_2 accumulation, but temperature and H_2 production/consumption-related genes were, respectively.

H_2 production pathways and genes under different temperatures

In order to verify the effect of H_2 consumption/production-related genes on H_2 accumulation, we calculated the abundance of each gene involved. As shown in Fig. 5, nine reactions involving H_2 production and consumption in HS-AD system were detected. Figure 5a, b, c and d shows the process of H_2 and $NADP^+$ reaction to generate NADPH, the process of catalytic H_2 to produce reduced receptors, the process of the reduced ferredoxin oxidized by H^+ to H_2, and the reduction of H^+ to H_2 by reduced ferredoxin catalyzed by coenzymes M and B, respectively. The genes involved in these reactions were detected in *Rhodococcus*, *Terrisporobacter*, *Ureibacillus* and *Bacteroides*. However, these genes were not enriched after HS-AD and were therefore not considered to be the main pathway regulating H_2 production and consumption. In addition, some major H_2 production pathways were detected as evident in Fig. 5e, f and g. Figure 5e shows the process of reducing H^+ to produce H_2. Only *mvhA*,

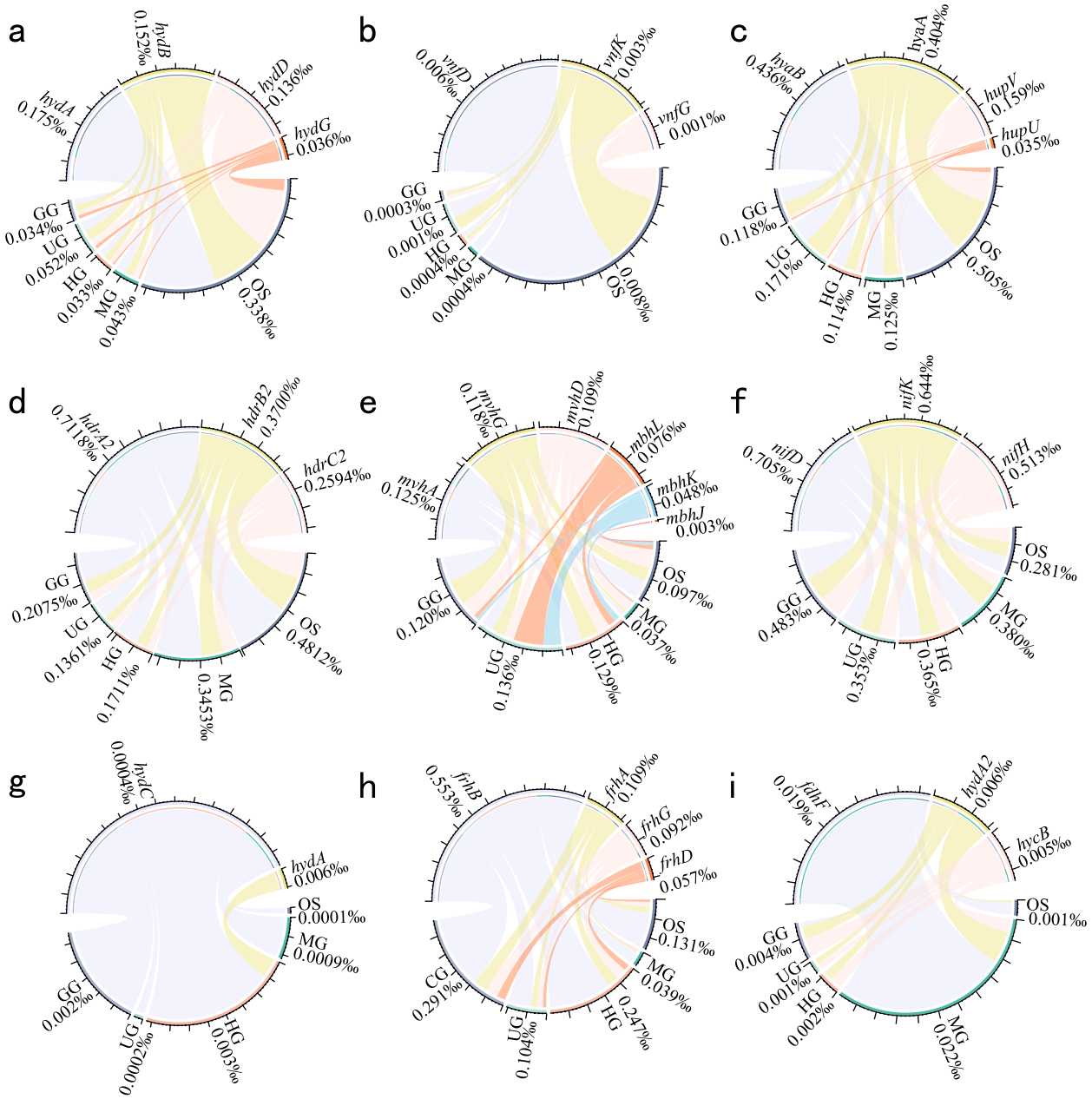

Fig. 5 The genes involved in reactions of the H_2 production and consumption process. **a** $H_2 + NADP^+ = H^+ + NADPH$, **b** H_2 + acceptor = reduced acceptor, **c** 12 reduced ferredoxin + 12 H^+ + N_2 + 40 ATP + 40 H_2O = 12 oxidized ferredoxin + 3 H_2 + 2 NH_3 + 40 ADP + 40 phosphate, **d** coenzyme B + coenzyme M + 2 reduced ferredoxin + 2 H^+ = coenzyme M 7-mercaptoheptanoylthreonine-phosphate heterodisulfide + 2 oxidized ferredoxin + 2 H_2, **e** 2 reduced ferredoxin + 2 H^+ = H_2 + 2 oxidized ferredoxin, **f** 8 reduced ferredoxin + 8 H^+ + N_2 + 16 ATP + 16 H_2O = 8 oxidized ferredoxin + H_2 + 2 NH_3 + 16 ADP + 16 phosphate, **g** 5 H^+ + NADH + 2 reduced ferredoxin = 2 H_2 + NAD^+ + 2 oxidized ferredoxin, **h** H_2 + oxidized coenzyme F_{420} = reduced coenzyme F_{420}, and **i** $CO_2 + H_2$ = formate

mvhG, *mbh* and *mbhK* were enriched during HS-AD, and these are considered to be main genes for H_2 production. Figure 5f shows that the three main genes involved in reducing H^+ to H_2 with ATP addition were *nifD*, *nifH* and *nifK*. Under constant temperature, the enrichment of *nifD* and *nifK* in MG was higher at 0.1600‰ and 0.1490‰, respectively, whereas in HG the *nifH*, *mvhA* and *mvhG* were more enriched at 0.1053‰, 0.0277‰ and 0.0295‰, respectively. The greater abundance of *mbhL* and *mbhK* in UG were 0.0495‰ and 0.0284‰, respectively. Therefore, the main H_2 production pathway of MG is likely to be the reaction given in Fig. 5e. Similarly, the

main H_2 production pathway for HG and UG were considered to be the reactions given in Fig. 5f. The genes *frhA*, *frhB*, *frhD* and *frhG* in Fig. 5g were involved in the formation of NADH, which is a H_2 production reaction. The total abundances of H_2 production-related genes in MG, HG and UG were 0.4105‰, 0.4672‰ and 0.4900‰, respectively, confirming the optimal H_2 production performance of UG. However, compared to constant temperature AD, the abundances of *nifD*, *nifH*, *nifK*, *mvhA* and *mvhG* of GG were higher, reaching 0.1849‰, 0.1467‰, 0.1519‰, 0.0405‰ and 0.0414‰, respectively. The reactions given in Fig. 5e and f both contributed the main H_2 production in GG. It is worth noting that the total abundance of H_2 production gene in GG was 0.6048‰, higher than that in UG, which was obviously inconsistent with the conclusion of H_2 production shown in Fig. 1. Perhaps these H_2 consumption-related genes were operating as regulators.

Two pathways and genes involved in H_2 consumption were also detected. Figure 5h shows the formation of reduced coenzyme F_{420} by the reduction of oxidized coenzyme F_{420} by H_2, and the enrichment of *hydC*. In Fig. 5i, three genes *fdhF*, *hydA2* and *hycB* were detected in the process of formate production from CO_2 and H_2. Compared to MG and UG, HG had a higher abundance of H_2 consumption gene (0.2494‰), and the total abundance of MG and UG was only 0.0605‰ and 0.1049‰. This indicates that the abundance order of H_2 consumption-related genes was HG > UG > MG. Although the abundance of H_2 consumption-related genes in HG and UG was higher than in MG, the H_2 accumulation in HG and UG was still more than in MG, indicating that hydrolysis and H_2 production-related genes together contribute to the high hydrogen production in UG. However, compared to UG, the total abundance of H_2 consumption-related genes detected in GG reached 0.2944‰, which was higher than in UG. The genes *frhA*, *frhB*, *frhD* and *frhG*, which were the most abundant genes, were regarded as the main H_2 consumption-related genes. Although GG had a high abundance of H_2 production-related genes, a high abundance of H_2 consumption-related genes led to more H_2 consumption, resulting in lower H_2 accumulation than UG. This supports the conclusion that HG produces more H_2 as evident in Fig. 1. It also confirmed the speculation in Fig. 3, that is, the high abundance of H_2-consuming bacteria and related genes led to the lowest H_2 accumulation.

As the above, although the abundance of H_2 production functional genes was dominant in gradient heating conditions (GG), the high enrichment of H_2 consumption-related genes (about 2.81 times higher than in UG) led to less actual H_2 production. The functional genes for H_2 production were mainly enriched in UG at 65 °C. Therefore, the H_2 accumulation was mainly affected by the enrichment of H_2-producing/consuming bacteria and related genes, which further addressed the question 2) in Fig. 3.

Significantly enriched functions in microbial systems

To explain why ultra-high temperature promotes lignin hydrolysis, we analyzed the significantly enriched functions of microbial communities. Linear discriminant analysis (LDA) scores can be used to assess key factors that contribute to sample differences due to high abundance [45]. Linear discriminant analysis effect size (LEfSe) analysis can also reveal the key pathways and modules under different temperature conditions by calculating LDA scores. The pathways and modules leading to sample differences with higher LDA scores are shown in Fig. 6, The enriched abundance of microbial metabolism in diverse environments, carbon metabolism, valine, leucine and isoleucine degradation, glyoxylate and dicarboxylate metabolism and fatty acid degradation was the reason for the difference in OS, indicating that the significant difference between OS and other samples was enriched, more diverse and active organic metabolic pathways. The biosynthesis of cofactors in MG was detected as the pathway with the highest contribution to the difference. The differences in HG were caused by ABC transporters, peptidoglycan biosynthesis and aminoacyl-tRNA, which indicated that the material transport and cell proliferation of microorganisms were more active at 55 °C. The differences in UG were the biosynthesis of secondary metabolites, flagella assembly, homologous recombination, pyridine metabolism and mismatch repair indicating that microbial movement, cell proliferation and microbial metabolism were more active under this condition. With the increase in temperature, the function of microbial movement, material transport and microbial metabolism under constant temperature is strengthened and considered the main reason for the difference, which confirms the speculation in Figs. 1d and 3 that the microbial reaction efficiency under ultra-high temperature is strengthened, which can promote the hydrolysis, acidogenic and H_2 production in UG. The main contribution to the difference in GG was attributed to the biosynthesis of amino acids, bacterial chemotaxis, amino sugar and nucleotide sugar metabolism, and starch and sucrose metabolism. Therefore, the advantage of UG at the pathway level was a more efficient microbial reaction and cellular processes promotion process, but this was not the case in GG. This is considered to be the main reason for the superior hydrolytic performance in UG, which addressed the question 1) in Fig. 3.

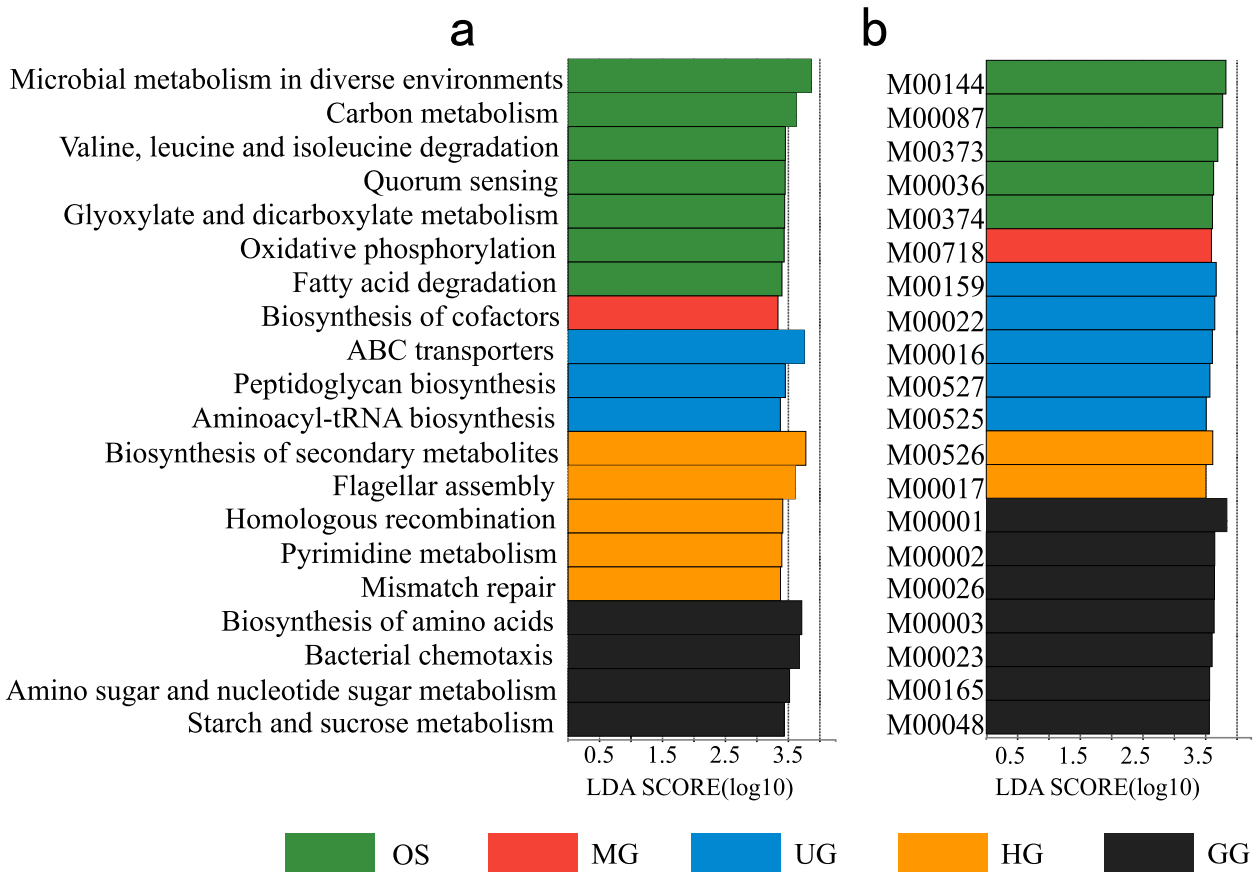

Fig. 6 Different levels of metabolic function cause differences between samples from different temperature conditions during HS-AD. **a** Top 20 pathways according to LDA scores, and **b** Top 20 modules according to LDA scores

Figure 6b shows that the OS enriched modules that contributed to the significant difference were NADH: quinone oxidoreductase (M00144), ethylmalonyl pathway (M00373), leucine degradation (M00036) in OS, which confirmed stong organic matter metabolic activity in OS. The enrichment of MG that caused the difference was multidrug resistance (M00718). Therefore, it was speculated the difference of the biosynthesis of cofactors of MG was mainly reflected in the drug resistance. The V/A-type ATPase (M00159), shikimate pathway (M00022) and three pathways involved in lysine synthesis (M00016, M00527 and M00525) were enriched in HG. The enriched pathways that contribute to the significant difference in UG were M00526 (lysine biosynthesis) and M00017 (methionine biosynthesis). Lysine and methionine are indispensable key amino acids in the metabolism of microorganisms, and the enrichment of their synthetic pathways indicates that the activity of microorganisms was enhanced [46]. The similarities between 55 and 65 °C were lysine enrichment, which was also different from the samples under other conditions. The enriched pathways in GG were glycolysis (M00001 and M00002), histidine biosynthesis (M00026), gluconeogenesis (M00003) and tryptophan biosynthesis (M00023), which together contributed to the significant difference. The enrichment of the glycolytic module confirmed was consistent with its superior acidogenic properties evident in Fig. 1d. The key histidine protein kinases for histidine biosynthesis is involved in a component of the two-component system [47], and GG can regulate adaptability of microorganisms to temperature through the enrichment of the two-component system, with the enrichment of organic matter metabolic modules. Compared to UG (24.26‰), the function of the two-component system enriched in GG (26.06‰) also confirms the enhancement of adaptive regulation. Enrichment of two-component system affected microbial metabolic processes, thus affecting community structure, which was considered to be one of the reasons for low environmental selection pressure in GG. Therefore, the higher the temperature was at constant temperature, the more lysine synthesis modules were enriched to improve the metabolic process. The two-component system regulated the microbial community to adapt to the condition of gradient heating, resulting in the

environmental selection pressure of GG being less than UG. Specifically, 65 °C promotes hydrolysis, acidogenic and H_2 production by enriching the functions involved in cellular processes and microbial metabolism. Under gradient heating conditions, community composition and function were regulated by an enriched two-component system, thus leading to less environmental selection pressure and lower enrichment in functional bacteria. Therefore, the main reason for the low environmental selection pressure in GG is the adaptive regulation contributed by the two-component system, which addressed the question 3) in Fig. 3.

According to the discussion, the mechanism of temperature regulating H_2 production can be summarized as follows. In the process of HS-AD producing H_2 from lignocellulose, temperature can regulate H_2 production by affecting lignin hydrolysis and H_2 accumulation (H_2 production/consumption-related genes), with the latter the limiting pathway. Under constant temperature in UG, in particular, the main reason for the higher hydrolytic performance was that the enhancement of microbial movement and cellular processes promoting lignin degradation. The enrichment of cellulose/hemicellulose degrading bacteria and related genes was another important reason. Also, the superior H_2 production in UG was mainly due to the inhibition of H_2-consuming bacteria and related genes at 65 °C and the enrichment of H_2 production-related genes. Notably, the H_2 production under gradient heating conditions, which we expected to have a higher potential, was lower than that under the constant 65 °C. As shown in Fig. 7, the difference of H_2 production mechanism between constant 65 °C and the gradient temperature conditions were clear. We found that the material transfer/transport was not enhanced under the

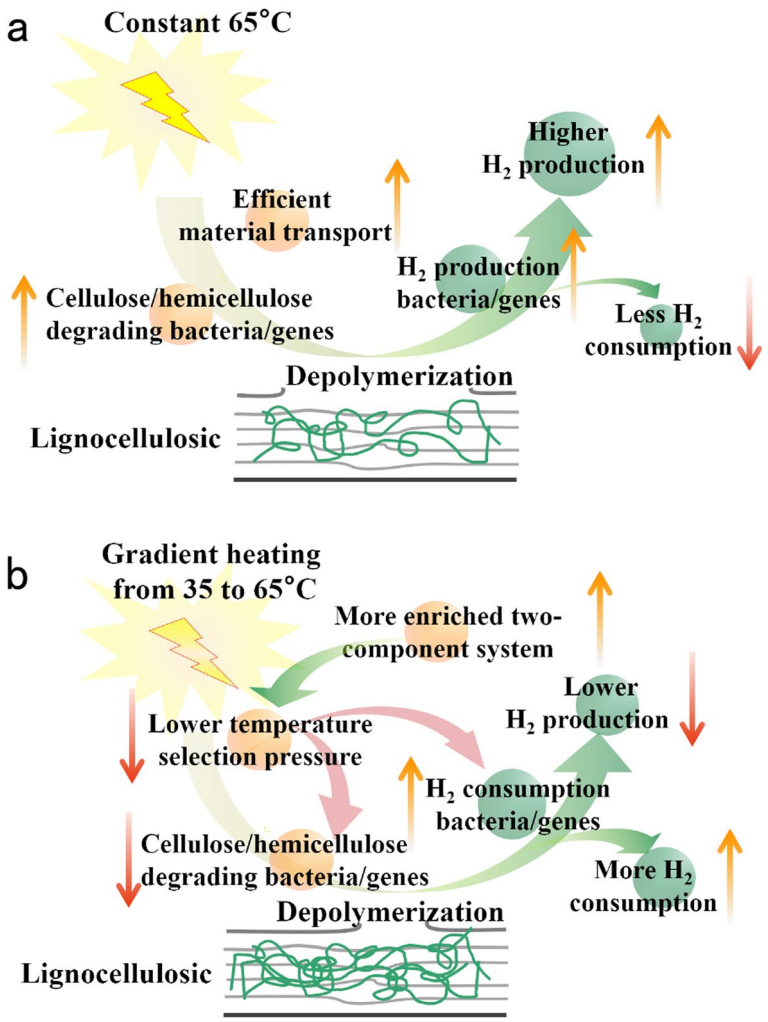

Fig. 7 Schematic comparison of H_2 accumulation regulation mechanisms under different temperature conditions. **a** Regulation of H_2 production under constant 65 °C, and **b** regulation of H_2 production under gradient heating conditions

gradient heating conditions in GG, and the regulation of two-component systems resulted in low environmental selection pressure and failed to enrich the ultra-high-temperature hydrolyzing bacteria, so that the lignocellulose hydrolytic performance was low. In addition, the H_2-consuming bacteria and related genes in GG were not inhibited, leading to lower H_2 accumulation.

Conclusions

We found that bacteria/genes contributing to H_2 production/consumption are the main contributors to H_2 accumulation, not the lignin degradation process. Also, the enrichment of functional pathway showed that the temperature enhanced the hydrolysis and H_2 production processes by promoting microbial material transfer and metabolic processes. In HS-AD of WS, under constant temperature (35, 55 and 65 °C), due to the enrichment of microbial movement and microbial metabolism at 65 °C, the high abundance of cellulose/hemicellulose hydrolysis bacteria/genes, the enrichment of H_2-producing bacteria and related genes, and the inhibition of H_2-producing/consuming bacteria and related genes, lignocellulose was easily deconstructed and degraded, and H_2 could be highly accumulated. Unexpectedly, the low abundance of ultra-high-temperature tolerant cellulose/hemicellulose hydrolytic bacteria/genes and enrichment of H_2 consumption-related genes led to decreased hydrolysis and H_2 production under gradient heating conditions (35 to 65 °C). This phenomenon was due to the regulation of two-component systems leading to weaker environmental selection pressure, resulting in microbial communities with reduced functionality compared to the communities at constant 65 °C. This work provides new insights into the mechanisms by which temperature can modulate H_2 production in HS-AD.

Abbreviations

HS-AD	High-solid anaerobic digestion
TS	Total solid
LS-AD	Liquid-state anaerobic digestion
WS	Wheat straw
TC	Total carbon
TN	Total nitrogen
VS	Volatile solid
WAS	Waste activated sludge
MG	Medium-temperature groups
HG	High-temperature groups
UG	Ultra-high temperature groups
GG	Gradient heating groups
OS	Original sample
EC	Electric conductivity
VFA	Volatile fatty acid
LE	Lignin esterase
Hase	[FeFe] hydrogenase
CrI	Crystallinity index
XRD	X-ray diffractometer
FT-IR	Fourier transform infrared spectroscopy
LDA	Linear Discriminant Analysis
LEfSe	Linear discriminant analysis effect size

Acknowledgements
We thank the wastewater treatment plant in Yangling District for providing waste activated sludge.

Authors' contributions
Heng Wu: Conceptualization, Methodology, Formal analysis, Investigation, Writing—original draft, Visualization. Huaiwen Zhang: Formal analysis, Visualization. Hongyi Lv: Methodology, Project administration. Caiyun Yang: Supervision. Anjie Li: Investigation. Suqi Li: Supervision. Yiqing Yao: Resources, Conceptualization, Supervision, Project administration, Writing, Review, Editing. All authors reviewed the manuscript.

Funding
This work was financially supported by the Shaanxi Youth Thousand Talents Project (A279021901), the Chinese Universities Scientific Fund (2452021112), the Shenzhen Natural Science Foundation (JCYJ20220530161408019), the Guangdong Provincial University Innovation Team Project (2023KCXTD038), the Shaanxi Provincial Department of Education Scientific Research Program (23JE015), the Foundation of State Key Laboratory of High-efficiency Utilization of Coal and Green Chemical Engineering (2022-K32), Northwest A&F University Young Talent Project (Z111021902).

Availability of data and materials
The metagenomic sequencing data of microbial samples at five temperature conditions have been were deposited to NCBI with project IDs of PRJNA897103.

Declarations

Ethics approval and consent to participate
Not applicable.

Consent for publication
Not applicable.

Competing interests
The authors declare no competing interests.

Author details
[1]College of Mechanical and Electronic Engineering, Northwest A&F University, Yangling, Shaanxi 712100, People's Republic of China. [2]College of Grassland Agriculture, Northwest A&F University, Yangling, Shaanxi 712100, People's Republic of China. [3]College of Life Sciences, Northwest A&F University, Yangling, Shaanxi 712100, People's Republic of China.

Received: 31 October 2022 Accepted: 14 August 2024
Published online: 10 September 2024

References

1. Mackey B, Lindenmayer D. Fossil fuels' future. Science. 2014;345(6198):739–40.
2. Liu WJ, Li WW, Jiang H, Yu HQ. Fates of Chemical elements in biomass during its pyrolysis. Chem Rev. 2017;117(9):6367–98.
3. Ma S, Wang H, Li J, Fu Y, Zhu W. Methane production performances of different compositions in lignocellulosic biomass through anaerobic digestion. Energy. 2019;189:116190.
4. Wang Z, Wang Z, Xu G, Ren J, Wang H, Li J. Sustainability assessment of straw direct combustion power generation in China: From the environmental and economic perspectives of straw substitute to coal. J Clean Prod. 2020;273:122890.
5. Fagbohungbe MO, Komolafe AO, Okere UV. Renewable hydrogen anaerobic fermentation technology: Problems and potentials. Renew Sust Energ Rev. 2019;114:109340.
6. Kizito S, Jjagwe J, Mdondo SW, Nagawa CB, Bah H, Tumutegyereize P. Synergetic effects of biochar addition on mesophilic and high total solids anaerobic digestion of chicken manure. J Environ Manage. 2022;315:115192.

7. Kothari R, Pandey AK, Kumar S, Tyagi VV, Tyagi SK. Different aspects of dry anaerobic digestion for bio-energy: an overview. Renew Sust Energ Rev. 2014;39:174–95.
8. Pastor-Poquet V, Papirio S, Steyer JP, Trably E, Escudié R, Esposito G. High-solids anaerobic digestion model for homogenized reactors. Water Res. 2018;142:501–11.
9. Monlau F, Trably E, Barakat A, Hamelin J, Steyer JP, Carrere H. Two-stage alkaline–enzymatic pretreatments to enhance biohydrogen production from sunflower stalks. Environ Sci Technol. 2013;47(21):12591–9.
10. Loy ACM, Alhazmi H, Lock SSM, Yiin CL, Cheah KW, Chin BLF, et al. Life-cycle assessment of hydrogen production via catalytic gasification of wheat straw in the presence of straw derived biochar catalyst. Bioresour Technol. 2021;341:125796.
11. Park JH, Jin MH, Lee DW, Lee YJ, Song GS, Park SJ, et al. Sustainable low-temperature hydrogen production from lignocellulosic biomass passing through formic acid: combination of biomass hydrolysis/oxidation and formic acid dehydrogenation. Environ Sci Technol. 2019;53(23):14041–53.
12. Davidi L, Moraïs S, Artzi L, Knop D, Hadar Y, Arfi Y, et al. Toward combined delignification and saccharification of wheat straw by a laccase-containing designer cellulosome. P Natl Acad Sci. 2016;113(39):10854–9.
13. Minty JJ, Singer ME, Scholz SA, Bae CH, Ahn JH, Foster CE, et al. Design and characterization of synthetic fungal-bacterial consortia for direct production of isobutanol from cellulosic biomass. P Natl Acad Sci. 2013;110(36):14592–7.
14. Lin Q, De Vrieze J, Li C, Li J, Li J, Yao M, et al. Temperature regulates deterministic processes and the succession of microbial interactions in anaerobic digestion process. Water Res. 2017;123:134–43.
15. Liu Y, Qian Y, Yong X, Jia H, Wei P, Zhou J. Effects of granular activated carbon and temperature on the viscosity and methane yield of anaerobically digested of corn straw with different dry matter concentrations. Bioresour Technol. 2021;332:125109.
16. Zhang Q, Fan D, Pang X, Zhu W, Zhao J, Xu J. Effects of polyethylene microplastics on the fate of antibiotic resistance genes and microbial communities in anaerobic digestion of dairy wastes. J Clean Prod. 2021;292:125909.
17. Sattar A, Arslan C, Ji C, Sattar S, Umair M, Sattar S, et al. Quantification of temperature effect on batch production of bio-hydrogen from rice crop wastes in an anaerobic bio reactor. Int J Hydrog Energy. 2016;41(26):11050–61.
18. Chang NB, Wen D, McKenna AM, Wanielista MP. The impact of carbon source as electron donor on composition and concentration of dissolved organic nitrogen in biosorption-activated media for stormwater and groundwater co-treatment. Environ Sci Technol. 2018;52(16):9380–90.
19. Tang CC, Zhang BC, Yao XY, Zhou AJ, Liu W, Ren YX, et al. Insights into response mechanism of anaerobic digestion of waste activated sludge to particle sizes of zeolite. Bioresour Technol. 2023;385:129348.
20. He ZW, Wang F, Zou ZS, Tang CC, Zhou AJ, Liu W, et al. Recent advances and perspectives in roles of humic acid in anaerobic digestion of waste activated sludge. Chem Eng J. 2023;466:143081.
21. Adav SS, Ravindran A, Sze SK. Quantitative proteomic analysis of lignocellulolytic enzymes by Phanerochaete chrysosporium on different lignocellulosic biomass. J Proteomics. 2012;75:1493–504.
22. Zhang J, Chen J, Ma R, Kumar V, Tong YW, He Y, et al. Mesophilic and thermophilic anaerobic digestion of animal manure: Integrated insights from biogas productivity, microbial viability and enzymatic activity. Fuel. 2022;320:123990.
23. Wang D, Duan Y, Yang Q, Liu Y, Ni BJ, Wang Q, et al. Free ammonia enhances dark fermentative hydrogen production from waste activated sludge. Water Res. 2018;133:272–81.
24. Wei W, Huang QS, Sun J, Dai X, Ni B. Revealing the mechanisms of polyethylene microplastics affecting anaerobic digestion of waste activated sludge. Environ Sci Technol. 2019;53(16):9604–13.
25. Wei W, Huang QS, Sun J, Wang JY, Wu SL, Ni BJ. Polyvinyl chloride microplastics affect methane production from the anaerobic digestion of waste activated sludge through leaching toxic bisphenol-A. Environ Sci Technol. 2019;53(5):2509–17.
26. Chirania P, Holwerda EK, Giannone RJ, Liang X, Poudel S, Ellis JC, et al. Metaproteomics reveals enzymatic strategies deployed by anaerobic microbiomes to maintain lignocellulose deconstruction at high solids. Nat Commun. 2022;13(1):3870.
27. Arenas CB, González R, González J, Cara J, Papaharalabos G, Gómez X, et al. Assessment of electrooxidation as pre- and post-treatments for improving anaerobic digestion and stabilisation of waste activated sludge. J Environ Manage. 2021;288:112365.
28. Marynowska M, Goux X, Sillam-Dussès D, Rouland-Lefèvre C, Halder R, Wilmes P, et al. Compositional and functional characterisation of biomass-degrading microbial communities in guts of plant fibre- and soil-feeding higher termites. Microbiome. 2020;8(1):96.
29. Shi H, Chen D, Jiang X, Li Y, Fan W, Hou C, et al. Simultaneous high-concentration pyridine removal and denitrification in an electricity assisted bio-photodegradation system. Chem Eng J. 2022;430:132598.
30. Arif M, Wang K, Zhu G, Li X, Lv Y, Piao DM, et al. Promoting direct interspecies electron transfer for methane production in bioelectrochemical anaerobic digestion: Impact of electrode surface area and switching circuit. Int J Hydrog Energy. 2022;47(52):21984–96.
31. Yang B, Lin Z, Liu Y, Hu D, Zhou X, Pan Q, et al. Spatial dynamics of biochemical fractions degradation, functional enzymatic activity and bacterial community within co-bioevaporation pile. J Clean Prod. 2021;287:125552.
32. Chen Y, Ping Q, Li D, Dai X, Li Y. Comprehensive insights into the impact of pretreatment on anaerobic digestion of waste active sludge from perspectives of organic matter composition, thermodynamics, and multi-omics. Water Res. 2022;226:119240.
33. Saha S, Jeon BH, Kurade MB, Govindwar SP, Chatterjee PK, Oh SE, et al. Interspecies microbial nexus facilitated methanation of polysaccharidic wastes. Bioresour Technol. 2019;289:121638.
34. Zakaria BS, Dhar BR. Intermittent energization catalyzes direct interspecies electron transfer in electro-anaerobic digestion of sewage sludge. Chem Eng J. 2022;442:136177.
35. Wang P, Li X, Chu S, Su Y, Wu D, Xie B. Metatranscriptomic insight into the effects of antibiotic exposure on performance during anaerobic co-digestion of food waste and sludge. J Hazard Mater. 2022;423:127163.
36. Xing T, Wang Z, Zhen F, Liu H, Wo D, Li L, et al. Initial pH-driven production of volatile fatty acid from hybrid Pennisetum. Bioresour Technol. 2022;347:126426.
37. Guan R, Yuan H, Zhang L, Zuo X, Li X. Combined pretreatment using CaO and liquid fraction of digestate of rice straw: anaerobic digestion performance and electron transfer. Chin J Chem Eng. 2021;36:223–32.
38. Bertin L, Lampis S, Todaro D, Scoma A, Vallini G, Marchetti L, et al. Anaerobic acidogenic digestion of olive mill wastewaters in biofilm reactors packed with ceramic filters or granular activated carbon. Water Res. 2010;44(15):4537–49.
39. Wang S, Zeng D, Jin B, Su Y, Zhang Y. Deciphering the role of polyethylene microplastics on antibiotic resistance genes and mobile genetic elements fate in sludge thermophilic anaerobic digestion process. Chem Eng J. 2023;452:139520.
40. Yan M, Treu L, Campanaro S, Tian H, Zhu X, Khoshnevisan B, et al. Effect of ammonia on anaerobic digestion of municipal solid waste: Inhibitory performance, bioaugmentation and microbiome functional reconstruction. Chem Eng J. 2020;401:126159.
41. Nie E, He P, Zhang H, Hao L, Shao L, Lü F. How does temperature regulate anaerobic digestion? Renew Sust Energ Rev. 2021;150:111453.
42. Hao Z, Yang B, Jahng D. Spent coffee ground as a new bulking agent for accelerated biodrying of dewatered sludge. Water Res. 2018;138:250–63.
43. Duan N, Kougias PG, Campanaro S, Treu L, Angelidaki I. Evolution of the microbial community structure in biogas reactors inoculated with seeds from different origin. Sci Total Environ. 2021;773:144981.
44. Niu Q, Takemura Y, Kubota K, Li YY. Comparing mesophilic and thermophilic anaerobic digestion of chicken manure: Microbial community dynamics and process resilience. Waste Manage. 2015;43:114–22.

45. Wu H, Zhang Q, Chen X, Wang L, Luo W, Zhang Z, et al. Effect of HRT and BDPs types on nitrogen removal and microbial community of solid carbon source SND process treating low carbon/nitrogen domestic wastewater. J Water Process Eng. 2021;40:101854.
46. Li W, Ma L, Shen X, Wang J, Feng Q, Liu L, et al. Targeting metabolic driving and intermediate influx in lysine catabolism for high-level glutarate production. Nat Commun. 2019;10(1):3337.
47. Buschiazzo A, Trajtenberg F. Two-component sensing and regulation: How do histidine kinases talk with response regulators at the molecular level? Annu Rev Microbiol. 2019;73(1):507–28.

Publisher's Note